



Multi-point scanning confocal Raman spectroscopy for accurate identification of microorganisms at the single-cell level

Yu Wang^{a,b}, Hao Peng^{a,b}, Kunxiang Liu^{a,b}, Lindong Shang^{a,b}, Lei Xu^c, Zhenming Lu^c, Bei Li^{a,b,*}

^a State Key Laboratory of Applied Optics, Changchun Institute of Optics, Fine Mechanics and Physics, Chinese Academy of Sciences, Changchun, 130033, PR China

^b University of Chinese Academy of Sciences, Beijing, 100049, PR China

^c National Engineering Research Center for Cereal Fermentation and Food Biomanufacturing, Jiangnan University, Wuxi, 214122, PR China

ARTICLE INFO

Keywords:

Multi-point scanning Raman spectroscopy
Microorganisms
Spatial heterogeneity
Single-cell level
Identification

ABSTRACT

Raman spectroscopy has been widely used for microbial analysis due to its exceptional qualities as a rapid, simple, non-invasive, reproducible, and real-time monitoring tool. The Raman spectrum of a cell is a superposition of the spectral information of all biochemical components in the laser focus. In the case where the microbial size is larger than the laser spot size, the Raman spectrum measured from a single-point within a cell cannot capture all biochemical information due to the spatial heterogeneity of microorganisms. In this work, we have proposed a method for the accurate identification of microorganisms using multi-point scanning confocal Raman spectroscopy. Through an image recognition algorithm and the control of a high-precision motorized stage, Raman spectra can be integrated at one time to measure the multi-point biochemical information of microorganisms. This solves the problem that the measured single microbial cells are of different sizes, and the laser spot of the confocal Raman system is not easy to change. Here, the single-cell Raman spectra of three *Escherichia coli* and seven *Lactobacillus* species were measured separately. The commonly used supervised classification method, support vector machine (SVM), was applied to compare the data based on the single-point spectra and multi-point scanning spectra. Multi-point spectra showed superior performance in terms of their accuracy and recall rates compared with single-point spectra. The results show that multi-point scanning confocal Raman spectra can be used for more accurate species classification at different taxonomic levels, which is of great importance in species identification.

1. Introduction

Rapid and reliable detection and identification of microorganisms are recognized as being critical in many modern microbiology laboratories. It has significant impacts in the fields of medical diagnostics, environmental science, and food safety. In the field of medical diagnostics, antimicrobial resistance is a global problem in pathogenic microorganisms, resulting in a high rate of illness and mortality. To enable earlier prescription of targeted medicines and help limit antimicrobial resistance, new technologies for quick, culture-free detection of bacterial infections are required [1–3]. To avoid spoiled and contaminated products during the production process before transferring to markers, the food industry requires a rapid-testing process. As a result, one of the most important steps in food quality control is

bacterial detection [4–6]. Detection and identification of bacteria are also crucial in environmental science, such as the detection of plant pathogens in agriculture [7–9], and the detection of extremophiles, such as bioweapons [10]. Raman spectroscopy is currently being promoted as a hot and ambitious technology that possesses all of the necessary characteristics for characterizing and identifying microorganisms [11–13]. Raman spectroscopy combined with confocal spectroscopy can interrogate individual microbial cells [14]. Confocal Raman spectroscopy is now widely used in microbiology, by means of high signal-to-noises Raman spectroscopy of individual microbial cells measured at a single point. In conjunction with comprehensive statistical analysis, Raman spectroscopy can achieve rapid, simple, reproducible, and non-invasive detection and identification of microorganisms [15–17]. For example, single-cell Raman spectroscopy

* Corresponding author. State Key Laboratory of Applied Optics, Changchun Institute of Optics, Fine Mechanics and Physics, Chinese Academy of Sciences, Changchun, 130033, PR China.

E-mail address: beili@ciomp.ac.cn (B. Li).

<https://doi.org/10.1016/j.talanta.2022.124112>

Received 26 August 2022; Received in revised form 7 November 2022; Accepted 16 November 2022

Available online 23 November 2022

0039-9140/© 2022 The Authors. Published by Elsevier B.V. This is an open access article under the CC BY-NC-ND license (<http://creativecommons.org/licenses/by-nc-nd/4.0/>).

coupled with heavy water labeling for rapid antibiotic susceptibility testing of pathogenic bacteria [18,19], detection of microorganisms in the ocean [20,21], and detection of food-borne microorganisms in meat and milk [22–25]. Furthermore, single-cell Raman spectroscopy is combined with gene sequencing, which can link phenotypic information of cells to their biological functions and gene expression, making biological research and application more beneficial [26–28].

Different microbial phenotypes have different molecular compositions, which results in subtle differences in their Raman spectra. It is well known that even the structure of individual microbial cells at the micron level contains molecular structures with different functions, such as nucleoid, ribosome, plasmid, mesosome, etc., which are randomly distributed inside the cell, i.e., the spatial heterogeneity of microorganisms. Barzand et al. [29] measured hyperspectral images of a single *Escherichia coli* cell (the laser spot-size of approximately 0.45 μm) in a scanning area of about $6 \times 5 \mu\text{m}$ and investigated the bacterium biological status at a subcellular level. The DNA segregation and Z-ring formation of a replicating bacterial cell were detected at a sub-micrometer level by multivariate data analysis. This suggests that there are differences in Raman spectra between regions within the bacteria. The confocal feature in confocal Raman spectroscopy enables the measurement of “point-to-point” Raman spectral information of the measured substance. The Raman spectrum of a cell is a superposition of the spectral information of all biochemical components in the laser focus [13]. Ho et al. [30] measured the majority of spectra on true monolayers and arise from ~ 1 cell due to the diffraction-limited laser spot size, which is roughly the size of a bacteria cell. Microorganisms vary in size, and the laser spot size is usually constant. The Raman spectrum of a cell is a superposition of the spectral information of all biochemical components in the laser focus. Due to the spatial heterogeneity of microorganisms, when the microbial size is larger than the laser spot size, the Raman spectrum measured from a single point within a cell cannot capture all biochemical information. It is worth mentioning that enabling the spectra to fully characterize the full biochemical information within a cell can also improve microbial identification accuracy, but this element is often overlooked.

In this work, we have developed a multi-point scanning measurement method for Raman spectra of a microbial cell by introducing an image recognition algorithm that can fully measure all biochemical components of microorganisms. The challenge that the measured single microbial cells are of different sizes and the laser spot of the confocal Raman equipment is not easily changed can be overcome. In conjunction with extensive statistical analysis, multi-point scanning confocal Raman spectra can be used to classify and identify species more accurately at different taxonomic levels.

2. Materials and methods

2.1. Sample preparation

In this work, three *Escherichia coli* species of the *Escherichia* and seven *Lactobacillus* species of the *Lactobacillus* were selected. In addition, we also used *Bacillus subtilis* and *Saccharomyces cerevisiae*. All strains of *Lactobacillus* were kindly provided by Grain Fermentation and Food Biomanufacturing, Jiangnan University. The three *Escherichia coli* species were *Escherichia coli* DH5 α (labeled *E. coli* 1), *Escherichia coli* BL21 (labeled *E. coli* 2), and *Escherichia coli* pcDNA3.1 (labeled *E. coli* 3), and seven *Lactobacillus* species were *Lactobacillus. acidophilus* (*L. acidophilus*), *Lactobacillus. helveticus* (*L. helveticus*), *Lactobacillus. paracasei* (*L. paracasei*), *Lactobacillus. brevis* (*L. brevis*), *Lactobacillus. brucei* (*L. brucei*), *Lactobacillus. fermentium* (*L. fermentium*), and *Lactobacillus. pentosus* (*L. pentosus*).

Three species of *E. coli* and *Bacillus subtilis* were cultivated in Luria-Bertani (LB) liquid medium at 37 °C overnight. And *Saccharomyces cerevisiae* was cultivated in Yeast extract Peptone Dextrose (YPD) liquid medium at 37 °C overnight. Seven species of *Lactobacillus* were

cultivated in Man Rogosa Sharpe (MRS) liquid medium at 37 °C for about 12 h. Then, 1 mL of the culture was washed with sterilized water, and the cells were purified from the nutrient broth with centrifugation at 8000 rpm for 1.5 min, and the above process was repeated three times to remove impurities that might interfere with Raman detection. The culture was then diluted in deionized water, shaken for 1–2 min, then 1–2 μL of sample was spotted onto aluminum coated Raman slides and waited until air-dried to ensure that dispersed individual cells could be observed under a $100 \times /0.8$ NA air objective.

2.2. Data collection method

Raman system. Raman spectra from microorganisms were acquired with the confocal Raman spectrometer HOOKE P300 (Hooke Instrument Ltd., China) as shown in Fig. 1. The system was equipped with two diffraction gratings with groove densities of 600 g/mm and 1200 g/mm (spectral resolutions of 3–4 cm^{-1} and 1–2 cm^{-1} , respectively) and a CCD camera (1340 \times 100 pixel, PIXIS 100B, PI) that can be cooled to -75 °C. A solid-state laser (08-DPL, Cobolt) with a wavelength of 532 nm was used to excite the Raman signal. The $100 \times /0.8$ NA objective lens (Olympus) generate a diffraction-limited spot size, $\sim 1 \mu\text{m}$ in diameter. The scanning wave number range is 340–3750 cm^{-1} (600 g/mm diffraction grating) and 240–2000 cm^{-1} (1200 g/mm diffraction grating).

Raman spectroscopy data acquisition. We integrated an image processing technique into multi-point scanning confocal Raman spectroscopy. The test and analysis process are shown in Fig. 2. In this study, the microorganism recognition system consists of several pivotal steps. The input image is a microbial microscope image. Firstly, the colorful image should be transformed into a gray image. Secondly, the gray image should be transformed into a binary image. The threshold is automatically calculated according to the histogram of the gray image. Then the contour of the microorganism can be extracted from the binary image by the operators of mathematical morphology. Additionally, the contour central moments and second-order moments are calculated to determine the center of gravity and the principal direction of the contour. Finally, find multiple evenly spaced points on the line segment along the principal direction of the contour and report their coordinates.

A computer-controlled, high-precision motorized stage was utilized to place the focused sample (100 nm resolution). When measuring Raman spectra of individual cells, the coordinates of multiple points found within the microbe were communicated to the motorized stage by selecting the serial number of microorganisms to be tested. The motorized stage would cause the laser to scan multiple points within the microorganisms in a sequential manner, with the integration time at each point being determined by the total integration time and the number of points. The scattered photons emitted by the laser interacting with each point were received by the CCD detector, transformed to electrical charge, and stored in a capacitor before being digitized by an amplifier and saved in the computer. Multi-point scanning confocal Raman spectra of individual microbial cells will be produced as a result.

2.3. Data pre-processing and data analysis

The use of data pre-processing has been shown to improve the robustness of subsequent data analysis and species identification, as well as interpretability, and to reduce the dimension of experimental data, thereby reducing the amount of data calculation [19]. On the experimentally obtained Raman spectra, the following data pre-processing steps were performed sequentially: removal of cosmic rays, smoothing, baseline correction, and normalization. In order to eliminate the effects of sample thickness and laser power, the Raman spectral data after the above processing were normalized by normalizing the data by the area in the range of 400–1800 cm^{-1} , which covers almost all of the useful information from the sample [20,30].

In this study, we used the support vector machine (SVM) with the

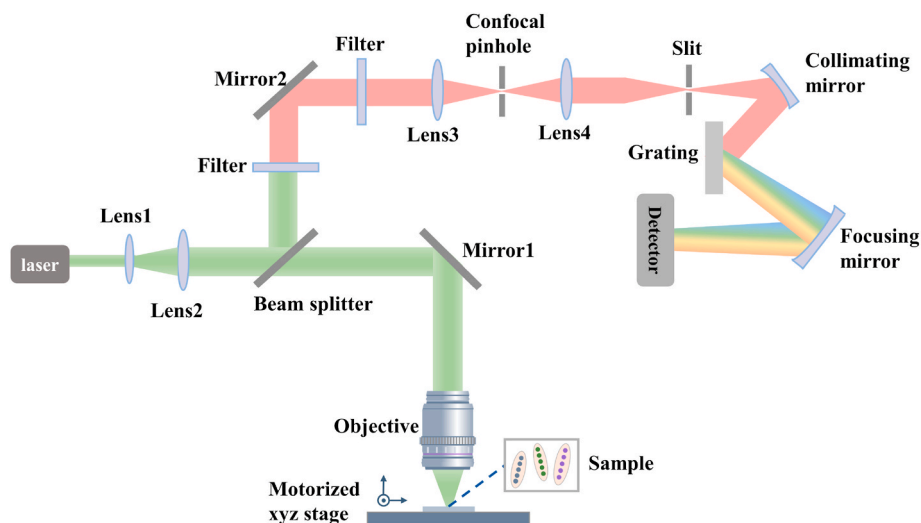


Fig. 1. Configuration of a confocal Raman micro-spectroscopy system.

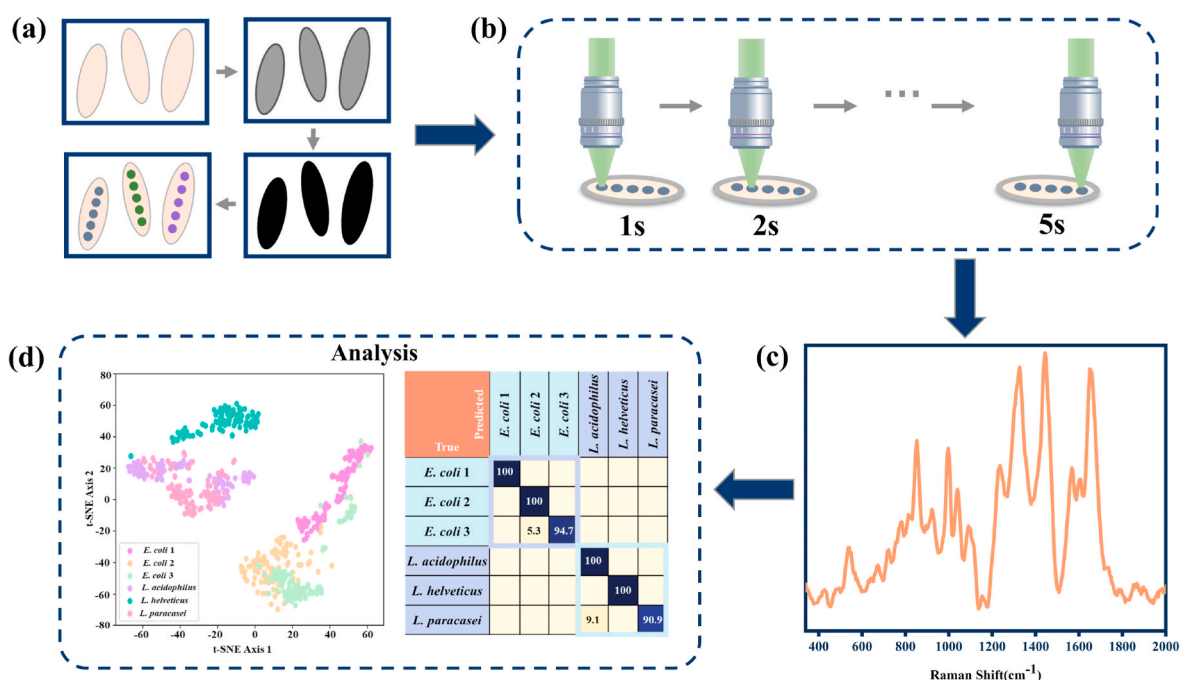


Fig. 2. Multi-point scanning confocal Raman spectroscopy measurements and analysis. (a) Microorganism recognition system. (b) Multi-point scanning Raman spectroscopy integration process. (c) A multi-point scanning confocal Raman spectrum. (d) Analysis of Raman spectral data.

radial basis kernel function as the classification for Raman spectral data. Based on the processed Raman spectral data, SVM models were developed and combined with the ten-fold cross-validation method to classify the species of 10 microorganisms.

3. Results and discussion

3.1. Detection of three different types of microorganisms using Raman mapping

Raman mapping collects Raman spectra from each pixel of a selected region, resulting in a 3D Raman hyperspectral image [31–33]. In this study, Raman mapping was used to collect and analyze data on three types of microorganisms: *E. coli*, *Bacillus subtilis*, and *Saccharomyces cerevisiae*. *E. coli* is a Gram-negative bacterium, *Bacillus subtilis* is a Gram-positive bacterium, and *Saccharomyces cerevisiae* is a fungus. The

microscope images are shown in Fig. 3a. Set the laser power to 5 mW and the single spectrum integration time to 3 s. Select an appropriate mapping region for a single cell. We measured an *E. coli* cell and a *Bacillus subtilis* cell in a scanning area of about $6 \times 6 \mu\text{m}$. The scanning area of a *Saccharomyces cerevisiae* cell was $6.6 \times 6.6 \mu\text{m}$. And the Raman mapping steps were both $0.3 \mu\text{m}$. Ensure that Raman spectra can be measured at all locations within a single microbial cell.

Fig. 3b shows Raman chemical images of the intensity of the strongest band of the three microbial Raman spectra at 2940 cm^{-1} , and this signal correlates to CH_2/CH_3 stretching. Fig. 3c focuses attention on the peak at 1449 cm^{-1} that is associated with $\delta(\text{CH}_2/\text{CH}_3)$ modes of C–H functional groups present in lipids, amino acid side chains of proteins, and carbohydrates. Fig. 3d shows the Raman chemical images at 780 cm^{-1} , with DNA as the primary source of signal. It can be seen that the Raman chemical images of the three microorganisms at the three wave numbers were nearly identical, but the intensity distribution differed

slightly. If the Raman spectra of microorganisms at different spatial locations are the same, the intensity distribution at various wave numbers should be identical. The difference in material composition information implied by the Raman spectra at the two positions of the two microorganisms is also shown in Fig. 3e and . This suggests that the Raman spectra of microorganisms at different spatial locations differ slightly due to their spatial heterogeneity. Different microorganism phenotypes are characterized by unique molecular compositions, but these differences are minute in Raman spectra, and the closer the relatives are to one another, the smaller the differences. Therefore, subtle differences in Raman spectra due to the spatial heterogeneity of microorganisms can affect the accuracy of identification when classifying different species of microorganisms.

3.2. Five-point scanning confocal Raman spectroscopy acquisition method

In this study, three *E. coli* species and seven *Lactobacillus* species were selected for Raman acquisition under a $100 \times /0.8$ NA objective. We observed that the cells in the field of view varied in size, and the majority of cells were around $3 \mu\text{m}$ in length. The selection of cell length was added to the microorganism recognition system described above, and we chose to test individual bacteria with a length of $2\text{--}5 \mu\text{m}$ in order to facilitate data acquisition. As previously stated, the laser spot size is approximately $1 \mu\text{m}$. To ensure that we can properly get information about the composition of individual bacterial cells, we set the number of identification points within the bacteria to 5.

We used two methods of Raman spectroscopy acquisition of bacteria and compared the results to see if full acquisition of the biochemical information of the bacteria is required for Raman spectroscopy-based bacterial identification. The first method is the traditional acquisition method, which selects a point in the center of the bacteria to measure Raman spectra, which is defined as a single-point spectrum. The second

acquisition method is the five-point scanning acquisition method, which is defined as a five-point scanning spectrum, identifies five points within the bacteria with equal spacing and scans them sequentially. As described in the Materials and Methods, a five-point scanning spectrum is a single spectrum obtained by controlling a high-precision motorized stage so that the laser is scanned sequentially to five positions within a single bacterium in a single uninterrupted exposure, rather than simply averaging five positions. In order to ensure the comparability of data, the integration conditions of both single-point and five-point scanning spectra were the same, the laser power was 5 mW, and the total integration time was 5 s (1 s for each point of the five-point scanning spectra). The data were not artificially screened during the acquisition process, and the number of Raman spectra acquired for each bacterium under both methods was about 100. The Raman spectra mean-variance plots are shown in Fig. 4, and the box plots of Raman spectra S/N ratios are shown in Fig. S1.

3.3. Data acquisition using grating with 600 g/mm

We chose the diffraction grating with 600 g/mm to collect data for three *E. coli* species and three *Lactobacillus* species (*L. acidophilus*, *L. helveticus* and *L. paracasei*). Three *E. coli* species are Gram-negative, while *Lactobacillus* species are Gram-positive. The confusion matrices of the 10-fold cross-validation were calculated for the SVM classification algorithms based on the single-point spectral data and five-point scanning spectral data.

Fig. 5 compares the SVM confusion matrices of the single-point spectral data with that of the five-point scanning spectral data. It indicates that the recall rates of various bacteria for the five-point scanning spectral data were higher than those of the single-point spectral data and that the recall rates of the five-point scanning spectral data were both greater than 90%. The classification accuracy of the SVM

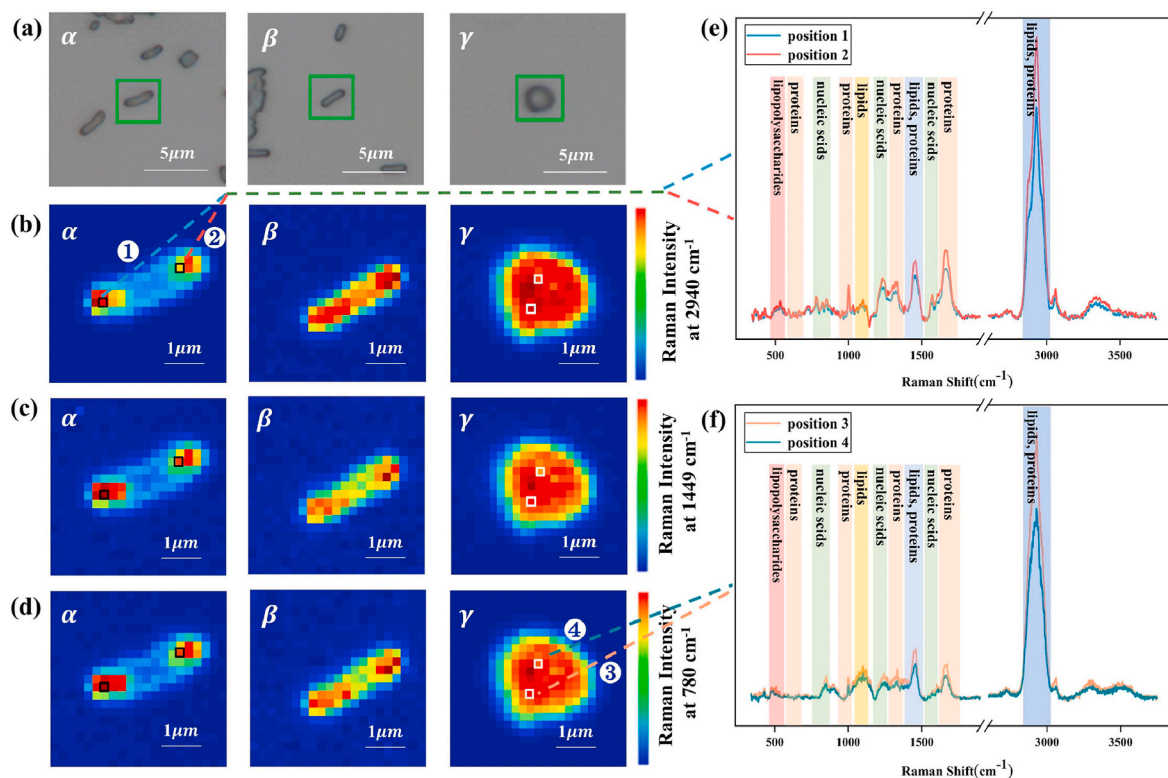


Fig. 3. (α) *E. coli*; (β) *Bacillus subtilis*; (γ) *Saccharomyces cerevisiae*; (a) Confocal microscope images of three microbial samples; (b) The Raman chemical images at 2940 cm^{-1} ; (c) The Raman chemical images at 1449 cm^{-1} ; (d) The Raman chemical images at 780 cm^{-1} ; (e) *E. coli* Raman spectra at positions 1 and 2, as well as the substances corresponding to the various peak positions; (f) The substances corresponding to the different peak positions in the Raman spectra of *Saccharomyces cerevisiae* at positions 3 and 4.

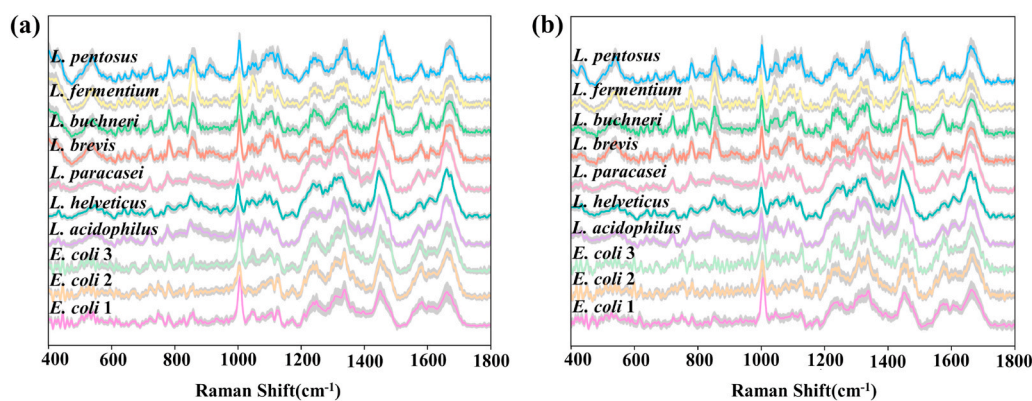


Fig. 4. Raman spectra mean-variance plots of single-point spectra (a) and five-point scanning spectra (b) for 10 microorganisms (Data for three *E. coli* species and three *Lactobacillus* species (*L. acidophilus*, *L. helveticus* and *L. paracasei*) were measured using the grating with 600 g/mm; Data for *L. brevis*, *L. bruchneri*, *L. fermentium* and *L. pentosus* were measured using the grating with 1200 g/mm. All data were interpolated and fitted with a wave number interval of 2 cm⁻¹ in the horizontal coordinate).

(a)	True	Predicted					
		<i>E. coli</i> 1	<i>E. coli</i> 2	<i>E. coli</i> 3	<i>L. acidophilus</i>	<i>L. helveticus</i>	<i>L. paracasei</i>
<i>E. coli</i> 1		95.7		4.3			
<i>E. coli</i> 2			100				
<i>E. coli</i> 3			5.6	94.4			
<i>L. acidophilus</i>					85.7		14.3
<i>L. helveticus</i>						100	
<i>L. paracasei</i>							88.9

(b)	True	Predicted					
		<i>E. coli</i> 1	<i>E. coli</i> 2	<i>E. coli</i> 3	<i>L. acidophilus</i>	<i>L. helveticus</i>	<i>L. paracasei</i>
<i>E. coli</i> 1		100					
<i>E. coli</i> 2			100				
<i>E. coli</i> 3			5.3	94.7			
<i>L. acidophilus</i>					100		
<i>L. helveticus</i>						100	
<i>L. paracasei</i>							90.9

Fig. 5. SVM confusion matrix of single-point spectra (a) and five-point scanning spectra (b) of six microorganisms measured using the grating with 600 g/mm (The number of single-point spectra and five-point scanning spectra is both 100 and the total integration time is both 5 s).

training model is defined by the proportion of data judged correctly by the model to the total data. The overall classification accuracy of the model was calculated to be $94.1 \pm 2.6\%$ and $97.6 \pm 1.7\%$ for the single-point spectral data and five-point scanning spectral data, respectively, an improvement in accuracy of approximately 3.7%. From the recall and classification accuracy of the SVM training model, the classification performance of the five-point scanning spectral data model was better than that of the single-point spectral data model.

We consider that it is due to the spatial heterogeneity within the bacteria and the fact that the laser spot size is smaller than the bacterial size. The single-point Raman spectra do not acquire all the information about individual bacterial cells, so the recall and accuracy of the single-point spectrum data model were low. The five-point scanning Raman spectra truly reflect the information of the sample itself, so the classification results of the five-point scanning Raman spectral data are more reasonable. Therefore, whether for Gram-negative or Gram-positive bacteria, it is more advantageous to fully acquire information about bacterial internal components and use multi-point scanning confocal Raman spectroscopy as data to build a database for bacterial classification analysis.

3.4. Data acquisition using grating with 1200 g/mm

In the above study, we used the 600 g/mm diffraction grating to demonstrate that multi-point scanning confocal Raman spectroscopy of bacteria is more advantageous for classification analysis. We reasoned that Raman spectra with high spectral resolution would make it easier to distinguish between single-point and five-point scanning spectra. Then we collected single-point and five-point scanning spectra of four

Lactobacillus species (*L. brevis*, *L. bruchneri*, *L. fermentium*, and *L. pentosus*) using a diffraction grating with 1200 g/mm for analysis and comparison.

As shown in Fig. 6a and Fig. 6b, for the single-point and five-point scanning spectra, the SVM classification algorithm was combined with the confusion matrix of the 10-fold cross-validation method. It can be seen that the recall rates of the five-point scanning spectral data were higher than those of the single-point spectral data, except for *L. brevis*. The overall classification accuracy of the SVM training model was $91.0 \pm 6.7\%$ for the single-point spectral data and $96.3 \pm 2.8\%$ for the five-point scanning spectral data, an improvement in accuracy of approximately 5.8%. For the five-point scanning spectral data, the SVM training model outperformed the single-point spectral data in terms of recall and classification accuracy.

As can be seen from the results, the improvement in recognition accuracy of the data measured using the 1200 g/mm grating is higher than that measured using the 600 g/mm grating. The data measured using the 1200 g/mm grating has a higher spectral resolution, making it easier to reveal differences between spectra. Therefore, the results measured using the 1200 g/mm grating reinforce the fact that spectral differences due to microbial spatial heterogeneity can affect the accuracy of species identification. Because of this, identifying different species of microorganisms is better suited to multi-point scanning spectroscopy, which accurately reflects the information of the sample itself.

As shown in Fig. S2 and Fig. S3, both K-Near Neighbor (KNN) and Linear Discriminant Analysis (LDA) training models for multi-point scanning spectra also show better classification results than single-point spectra. In addition, the *t*-SNE clustering results after feature

(a)	True	Predicted <i>L. brevis</i>	<i>L. buchneri</i>	<i>L. fermentium</i>	<i>L. pentosus</i>
<i>L. brevis</i>		94.7	5.3		
<i>L. buchneri</i>			73.9	26.3	
<i>L. fermentium</i>		4.5		95.5	
<i>L. pentosus</i>					100

(b)	True	Predicted <i>L. brevis</i>	<i>L. buchneri</i>	<i>L. fermentium</i>	<i>L. pentosus</i>
<i>L. brevis</i>		90	10		
<i>L. buchneri</i>			95	5	
<i>L. fermentium</i>				100	
<i>L. pentosus</i>					100

Fig. 6. SVM confusion matrix of single-point spectra (a) and five-point scanning spectra (b) of six microorganisms measured using the grating with 1200 g/mm (The number of single-point spectra and five-point scanning spectra is both 100 and the total integration time is both 5 s).

extraction for single-point spectral data and five-point scanning spectral data are plotted as shown in Fig. S4 and Fig. S5. We can intuitively see that the clustering results for the five-point scanning spectral data are closer to the real-life sample situation than the clustering results for the single-point spectra. In summary, multi-point scanning confocal Raman spectroscopy can better reveal the biochemical components of individual bacterial cells, whether using a diffraction grating with 600 g/mm or 1200 g/mm. They perform better in classification analyses and have a higher possibility of correctly identifying microbial species.

4. Conclusions

To address the spatial heterogeneity of microorganisms, we have proposed multi-point scanning confocal Raman spectroscopy based on an image processing technique. Then we compared the traditional acquisition method with the multi-point scanning acquisition method by using the SVM classification recognition algorithm. Multi-point scanning confocal Raman spectra had high recall rates (reaching 90%) and identification accuracy rates (~96%) compared to single-point Raman spectroscopy. The results indicate that multi-point scanning confocal Raman spectroscopy can fully characterize the full biochemical information within a cell, making the Raman spectrum a true “fingerprint spectrum” of individual cells. In conjunction with extensive statistical analysis, it enables the development of a more reliable Raman spectroscopy database of microorganisms. As a result, multi-point scanning confocal Raman spectroscopy has a lot of potential for use in microbial identification and classification, which would be beneficial to various fields of microbiology.

Credit authors statement

Yu Wang: Investigation, Software, Writing-Original draft, Writing-Review & Editing. **Hao Peng:** Data curation. **Kunxiang Liu and Lindong Shang:** Formal analysis. **Lei Xu:** Sample preparation. **Zhenming Lu:** Resources. **Bei Li:** Conceptualization.

Declaration of competing interest

The authors declare that they have no known competing financial interests or personal relationships that could have appeared to influence the work reported in this paper.

Data availability

The authors are unable or have chosen not to specify which data has been used.

Acknowledgements

This research did not receive any specific grant from funding agencies in the public, commercial, or not-for-profit sectors.

Appendix A. Supplementary data

Supplementary data to this article can be found online at <https://doi.org/10.1016/j.talanta.2022.124112>.

References

- [1] F. Prestinaci, P. Pezzotti, A. Pantosti, Antimicrobial resistance: a global multifaceted phenomenon, *Pathog. Glob. Health* 109 (2015) 309–318.
- [2] A. Potron, L. Poirel, P. Nordmann, Emerging broad-spectrum resistance in *Pseudomonas aeruginosa* and *Acinetobacter baumannii*: mechanisms and epidemiology, *Int. J. Antimicrob. Agents* 45 (2015) 568–585.
- [3] A.H. Holmes, L.S.P. Moore, A. Sundsfjord, M. Steinbakk, S. Regmi, A. Karkey, P. J. Guerin, L.J.V. Piddock, Understanding the mechanisms and drivers of antimicrobial resistance, *Lancet* 387 (2016) 176–187.
- [4] M. Pavlovic, I. Huber, R. Konrad, U. Busch, Application of MALDI-TOF MS for the identification of food borne bacteria, *Open Microbiol. J.* 7 (2013) 135–141.
- [5] S. Huayhongthong, P. Khuntayaporn, K. Thirapanmethee, P. Wanapaisan, M. T. Chomnawang, Raman spectroscopic analysis of food-borne microorganisms, *Lebensm. Wiss. Technol.* 114 (2019), 108419.
- [6] R. Breuch, D. Klein, E. Siefke, M. Hebel, U. Herbert, C. Wickleder, P. Kaul, Differentiation of meat-related microorganisms using paper-based surface-enhanced Raman spectroscopy combined with multivariate statistical analysis, *Talanta* 219 (2020), 121315.
- [7] I.A. Tikhonovich, N.A. Provorov, Microbiology is the basis of sustainable agriculture: an opinion, *Ann. Appl. Biol.* 159 (2011) 155–168.
- [8] S. Baruah, J. Dutta, Nanotechnology applications in pollution sensing and degradation in agriculture: a review, *Environ. Chem. Lett.* 7 (2009) 191–204.
- [9] Y. Fang, R.P. Ramasamy, Current and prospective methods for plant disease detection, *Biosensors* 5 (2015) 537–561.
- [10] R.J. Hawley, E.M. Eitzen Jr., Biological weapons—a primer for microbiologists, *Annu. Rev. Microbiol.* 55 (2001) 235–253.
- [11] R.R. Jones, D.C. Hooper, L. Zhang, D. Wolverson, V.K. Valev, Raman techniques: fundamentals and frontiers, *Nanoscale Res. Lett.* 14 (2019) 231.
- [12] S.P. Mulvaney, C.D. Keating, Raman spectroscopy, *Anal. Chem.* 72 (2000) 145R–157R.
- [13] B. Lorenz, C. Wichmann, S. Stockel, P. Rosch, J. Popp, Cultivation-free Raman spectroscopic investigations of bacteria, *Trends Microbiol.* 25 (2017) 413–424.
- [14] J. Müller, W. Ibach, K. Weishaupt, O. Hollricher, Confocal Raman microscopy, *Microsc. Micro* 9 (2003) 1084–1085.
- [15] S. Pahlow, S. Meisel, D. Cialla-May, K. Weber, P. Rosch, J. Popp, Isolation and identification of bacteria by means of Raman spectroscopy, *Adv. Drug Deliv. Rev.* 89 (2015) 105–120.
- [16] K. Maquelin, L.P. Choo-Smith, H.P. Endtz, H.A. Bruining, G.J. Puppels, Rapid identification of *Candida* species by confocal Raman microspectroscopy, *J. Clin. Microbiol.* 40 (2002) 594–600.
- [17] S. Lee, Z. Landry, F.C. Pereira, M. Wagner, D. Berry, W.E. Huang, G.T. Taylor, J. Kneipp, J. Popp, M. Zhang, J.X. Cheng, R. Stocker, Raman microspectroscopy for microbiology, *Nat. Rev. Methods Primers* 1 (2021).
- [18] K. Yang, H.Z. Li, X. Zhu, J.Q. Su, B. Ren, Y.G. Zhu, L. Cui, Rapid antibiotic susceptibility testing of pathogenic bacteria using heavy-water-labeled single-cell Raman spectroscopy in clinical samples, *Anal. Chem.* 91 (2019) 6296–6303.

- [19] Y. Tao, Y. Wang, S. Huang, P. Zhu, W.E. Huang, J. Ling, J. Xu, Metabolic-activity based assessment of antimicrobial effects by D₂O-labeled single-cell Raman microspectroscopy, *Anal. Chem.* 89 (2017) 4108–4115.
- [20] Y. Liu, J. Xu, Y. Tao, T. Fang, W. Du, A. Ye, Rapid and accurate identification of marine microbes with single-cell Raman spectroscopy, *Analyst* 145 (2020) 3297–3305.
- [21] B. Liu, K. Liu, N. Wang, K. Ta, P. Liang, H. Yin, B. Li, Laser tweezers Raman spectroscopy combined with deep learning to classify marine bacteria, *Talanta* 244 (2022), 123383.
- [22] S. Meisel, S. Stockel, P. Rosch, J. Popp, Identification of meat-associated pathogens via Raman microspectroscopy, *Food Microbiol.* 38 (2014) 36–43.
- [23] S. Meisel, S. Stockel, M. Elschner, F. Melzer, P. Rosch, J. Popp, Raman spectroscopy as a potential tool for detection of *Brucella* spp. in milk, *Appl. Environ. Microbiol.* 78 (2012) 5575–5583.
- [24] S. Yan, S. Wang, J. Qiu, M. Li, D. Li, D. Xu, D. Li, Q. Liu, Raman spectroscopy combined with machine learning for rapid detection of food-borne pathogens at the single-cell level, *Talanta* 226 (2021), 122195.
- [25] J. Neng, Q. Zhang, P. Sun, Application of surface-enhanced Raman spectroscopy in fast detection of toxic and harmful substances in food, *Biosens. Bioelectron.* 167 (2020), 112480.
- [26] D. Wang, P. He, Z. Wang, G. Li, N. Majed, A.Z. Gu, Advances in single cell Raman spectroscopy technologies for biological and environmental applications, *Curr. Opin. Biotechnol.* 64 (2020) 218–229.
- [27] M. Li, D.G. Boardman, A. Ward, W.E. Huang, Single-cell Raman sorting, *Methods Mol. Biol.* 1096 (2014) 147–153.
- [28] L. Cui, K. Yang, H.Z. Li, H. Zhang, J.Q. Su, M. Paraskevaidi, F.L. Martin, B. Ren, Y. G. Zhu, Functional single-cell approach to probing nitrogen-fixing bacteria in soil communities by resonance Raman spectroscopy with ¹⁵N₂ labeling, *Anal. Chem.* 90 (2018) 5082–5089.
- [29] G. Barzan, A. Sacco, L. Mandrile, A.M. Giovannozzi, C. Portesi, A.M. Rossi, Hyperspectral chemical imaging of single bacterial cell structure by Raman spectroscopy and machine learning, *Appl. Sci.* 11 (2021) 3409.
- [30] C.S. Ho, N. Jean, C.A. Hogan, L. Blackmon, S.S. Jeffrey, M. Holodniy, N. Banaei, A. A.E. Saleh, S. Ermon, J. Dionne, Rapid identification of pathogenic bacteria using Raman spectroscopy and deep learning, *Nat. Commun.* 1 (2019) 4927.
- [31] J. Hutchings, C. Kendall, B. Smith, N. Shepherd, H. Barr, N. Stone, The potential for histological screening using a combination of rapid Raman mapping and principal component analysis, *J. Biophot.* 2 (2009) 91–103.
- [32] K.C. Gordon, C.M. McGoverin, Raman mapping of pharmaceuticals, *Int. J. Pharm.* 417 (2011) 151–162.
- [33] A.A. Gowen, Y. Feng, E. Gaston, V. Valdramidis, Recent applications of hyperspectral imaging in microbiology, *Talanta* 137 (2015) 43–54.